Supporting Information

Interaction between the Heme and a G-quartet in a Heme-DNA Complex

Kaori Saito, Hulin Tai, Hikaru Hemmi,[+] Nagao Kobayashi,[*, %] and Yasuhiko Yamamoto[*]

Department of Chemistry, University of Tsukuba, Tsukuba 305-8571, Japan, [+]National Food Research Institute, National Agriculture and Food Research Organization (NARO), Tsukuba 305-8642, Japan, and [%]Department of Chemistry, Graduate School of Science, Tohoku University, Sendai 980-8578, Japan

Corresponding author:
Yasuhiko Yamamoto
E-mail address: yamamoto@chem.tsukuba.ac.jp
Phone and Fax: +81-29-853-6521

Nagao Kobayashi
E-mail address: nagaok@m.tohoku.ac.jp
Phone and Fax: +81-22-795-7719

Table S1. Chemical shifts (ppm) and chemical shift changes, Δδ (ppm), of the ^{1}H NMR signals of $(d(TTAGGG))_4$ in 90%$^{1}H_2O$/10%$^{2}H_2O$, 300 mM KCl, 50 mM potassium phosphate buffer at pH 9.80 and 7.00, and 25 ºC.

Chemical shift δ (ppm)

	H1'		H2'/H2"		H3'		H4'		H5'/H5"		H6/H8		NH/Me/H2	
	pH 9.80	pH 7.00[a]	pH 9.80	pH 7.00[a]	pH 9.80	pH 7.00[a]	pH 9.80	pH7.00[a]	pH 9.80	pH 7.00[a]	pH 9.80	pH 7.00[a]	pH 9.80	pH 7.00[a]
T1	5.95	5.92	2.03, 2.27	2.02, 2.28	4.58	4.59	3.94	3.94	3.57, 3.62	—	7.31	7.34	1.62	1.62
T2	6.15	6.12	1.97, 2.25	1.98, 2.27	4.66	4.68	4.00	4.01	—	—	7.22	7.23	1.70	1.68
A3	6.19	6.19	2.82	2.82	5.01	5.01	4.39	4.39	4.03, 4.09	—	8.31	8.32	7.99	8.00
G4	5.96	5.97	2.52, 2.83	2.52, 2.83	4.92	4.92	4.45	4.46	—	—	7.72	7.72	11.23	11.24
G5	6.04	6.03	2.64, 2.82	2.65, 2.81	4.98	4.98	4.42	4.42	—	—	7.43	7.43	10.84	10.84
G6	6.05	6.05	2.55, 2.78	2.56, 2.78	4.80	4.80	4.26	4.26	—	—	7.28	7.29	10.46	10.46

Δδ [b] (ppm)

T1	0.03	0.01, -0.01	-0.01	0.00	—	-0.03	0.00
T2	0.03	-0.01, -0.02	-0.02	-0.01	—	-0.01	0.02
A3	0.00	0.00	0.00	0.00	—	-0.01	-0.01
G4	0.01	0.00, 0.00	0.00	-0.01	—	0.01	-0.01
G5	-0.01	-0.01, 0.01	-0.01	0.00	—	0.00	0.00
G6	0.00	-0.01, 0.00	0.00	0.00	—	-0.01	0.00

[a] Taken from Mita, H.; Ohyama, T.; Tanaka, Y.; Yamamoto, Y. *Biochemistry*, **2006**, *22*, 6765-6772.

[b] $\Delta\delta = \delta_{\text{pH 9.80}} - \delta_{\text{pH 7.00.}}$

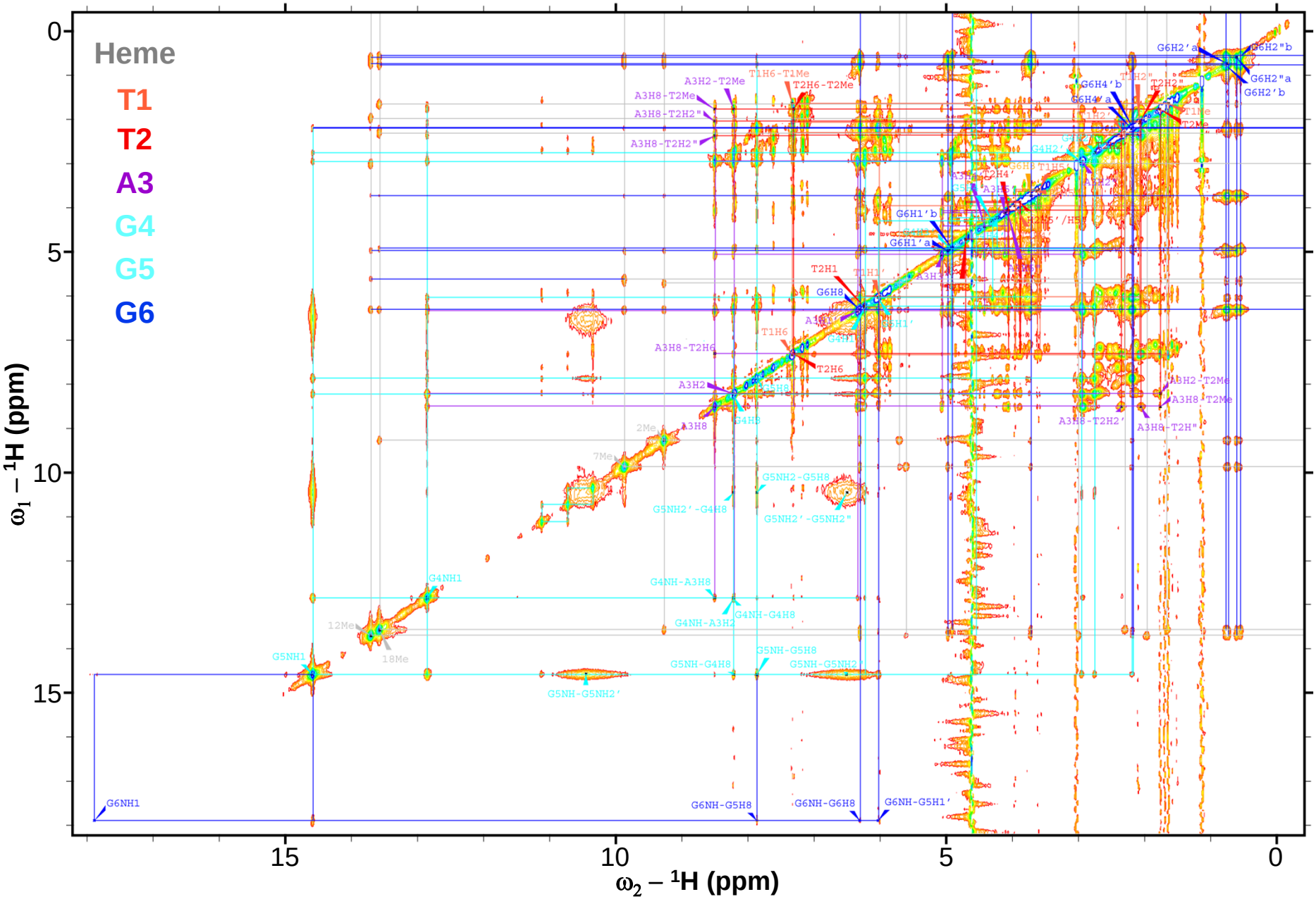

Figure S1. A portion of the NOESY spectrum of the heme(Fe^{3+})-$(d(TTAGGG))_4$ complex in 90%^1H_2O/10%^2H_2O, 300 mM KCl, 50 mM potassium phosphate buffer at pH 9.80 and 25 ºC. A mixing time of 150 ms was used to record the spectrum. The connectivities used for signal assignments are indicated in the spectrum.

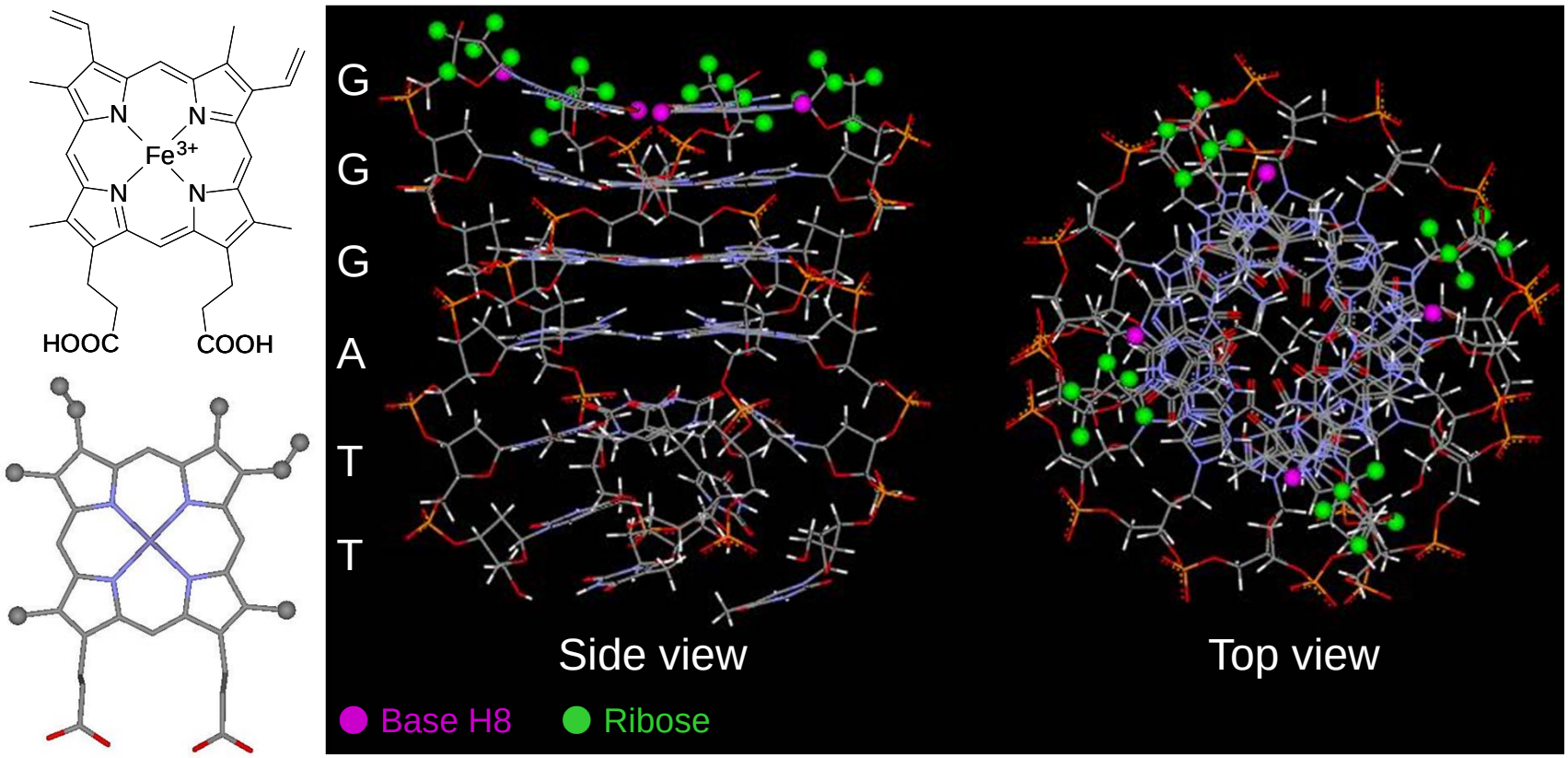

Figure S2. Schematic representation of intermolecular NOEs observed between the heme(Fe^{3+}) and $(d(TTAGGG))_4$ in the complex. The G6 (H8 (pink balls) and H1'- H4' (green balls)) protons of the complex exhibited NOE connectivities with the heme methyl and vinyl protons. The structure of $(d(TTAGGG))_4$ was taken from PDB entry 1NP9.

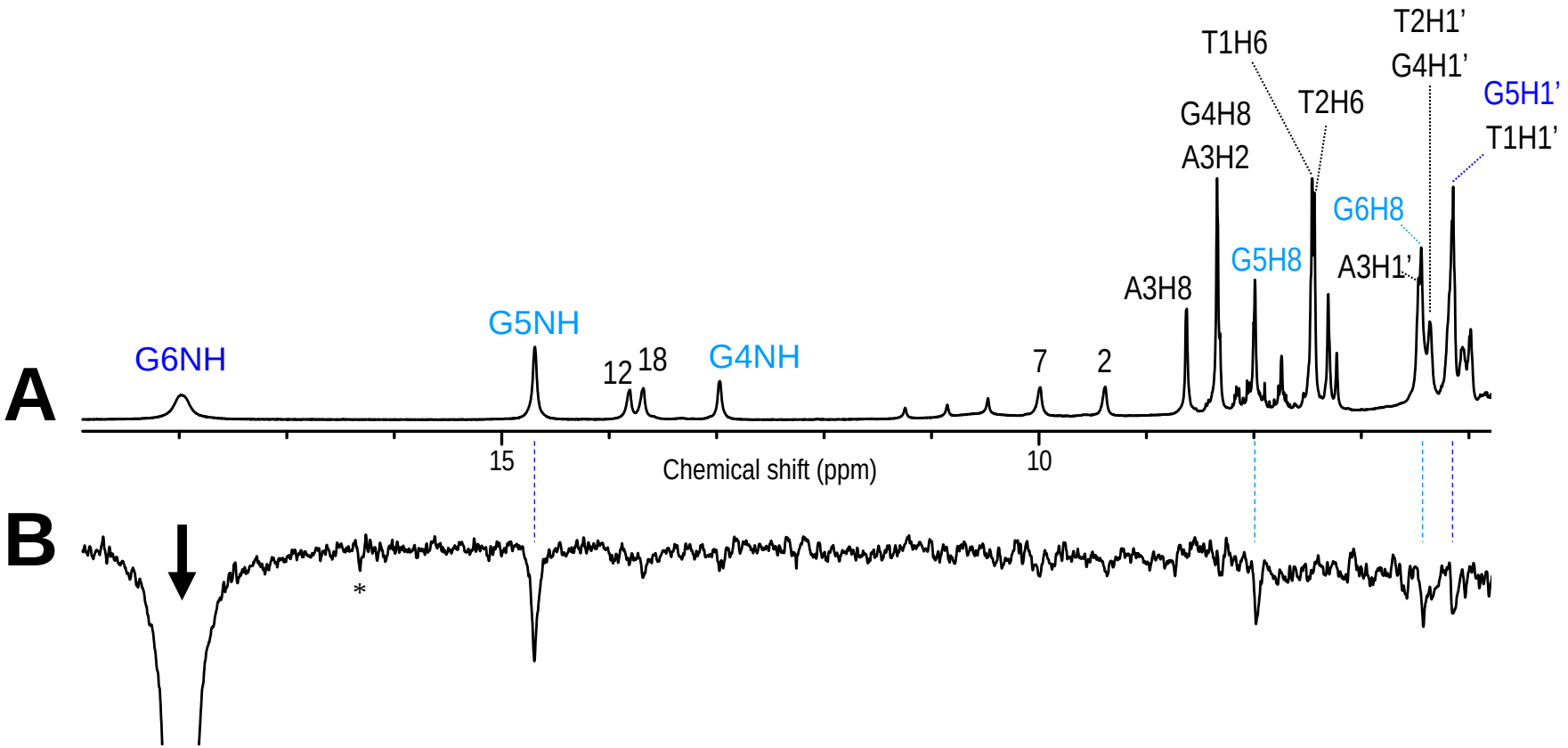

Figure S3. Nuclear Overhauser effect (NOE) difference spectrum of the heme(Fe^{3+})-$(d(TTAGGG))_4$ complex in 90%^1H_2O/10%^2H_2O, 300 mM KCl, 50 mM potassium phosphate buffer at pH 9.80 and 25 ºC. (A) Reference spectrum. (B) The NOE difference spectrum resulting from saturation of the G6 imino proton (G6NH) signal. The G5 imino proton (G5NH) signal and the ribose G5H8, G6H8, and G5H1' proton signals exhibited NOEs.

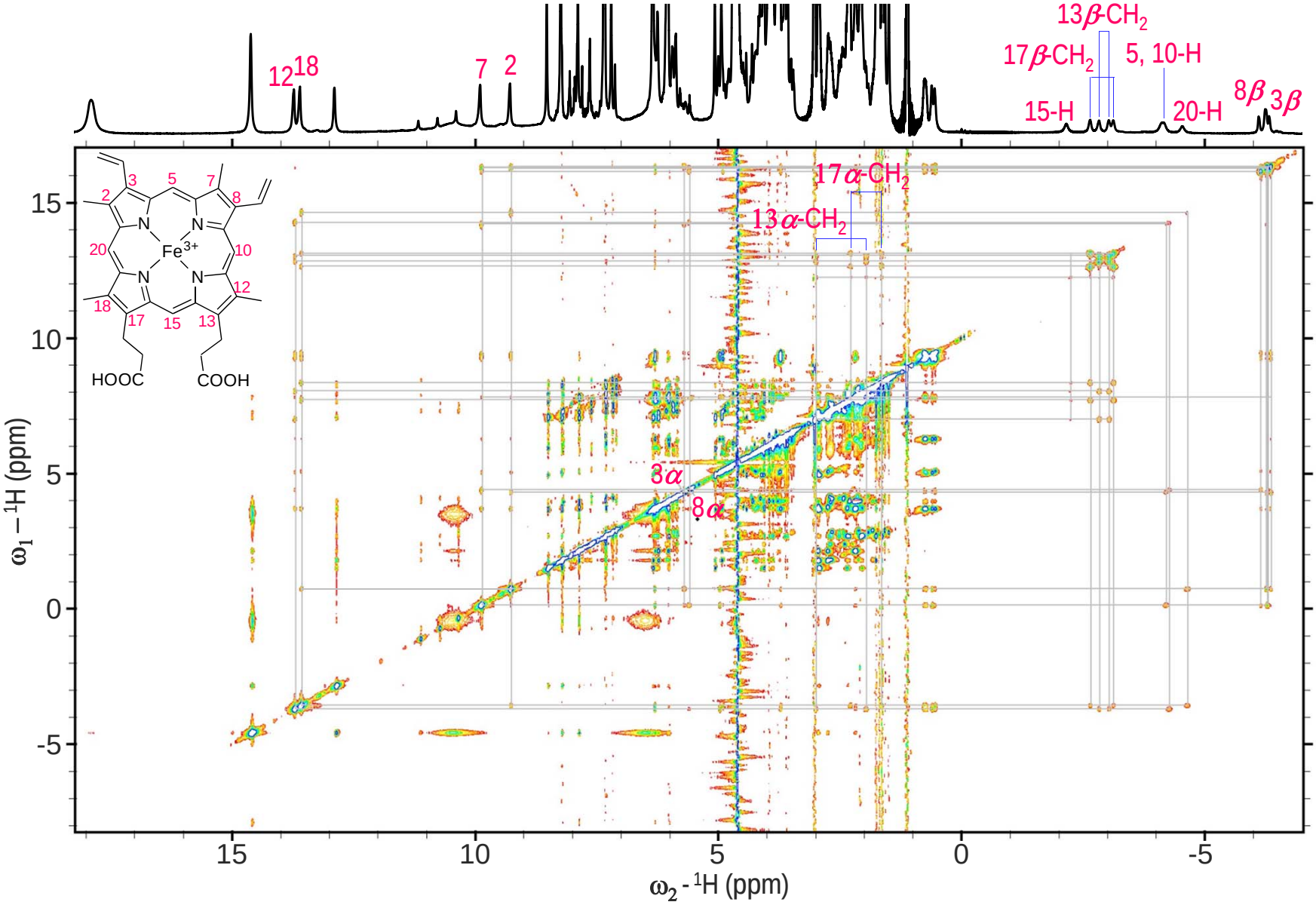

Figure S4. NOESY spectrum of the heme(Fe^{3+})-$(d(TTAGGG))_4$ complex in 90%^1H_2O/10%^2H_2O, 300 mM KCl, 50 mM potassium phosphate buffer at pH 9.80 and at 25 ºC. The spectrum was recorded using a mixing time of 150 ms.

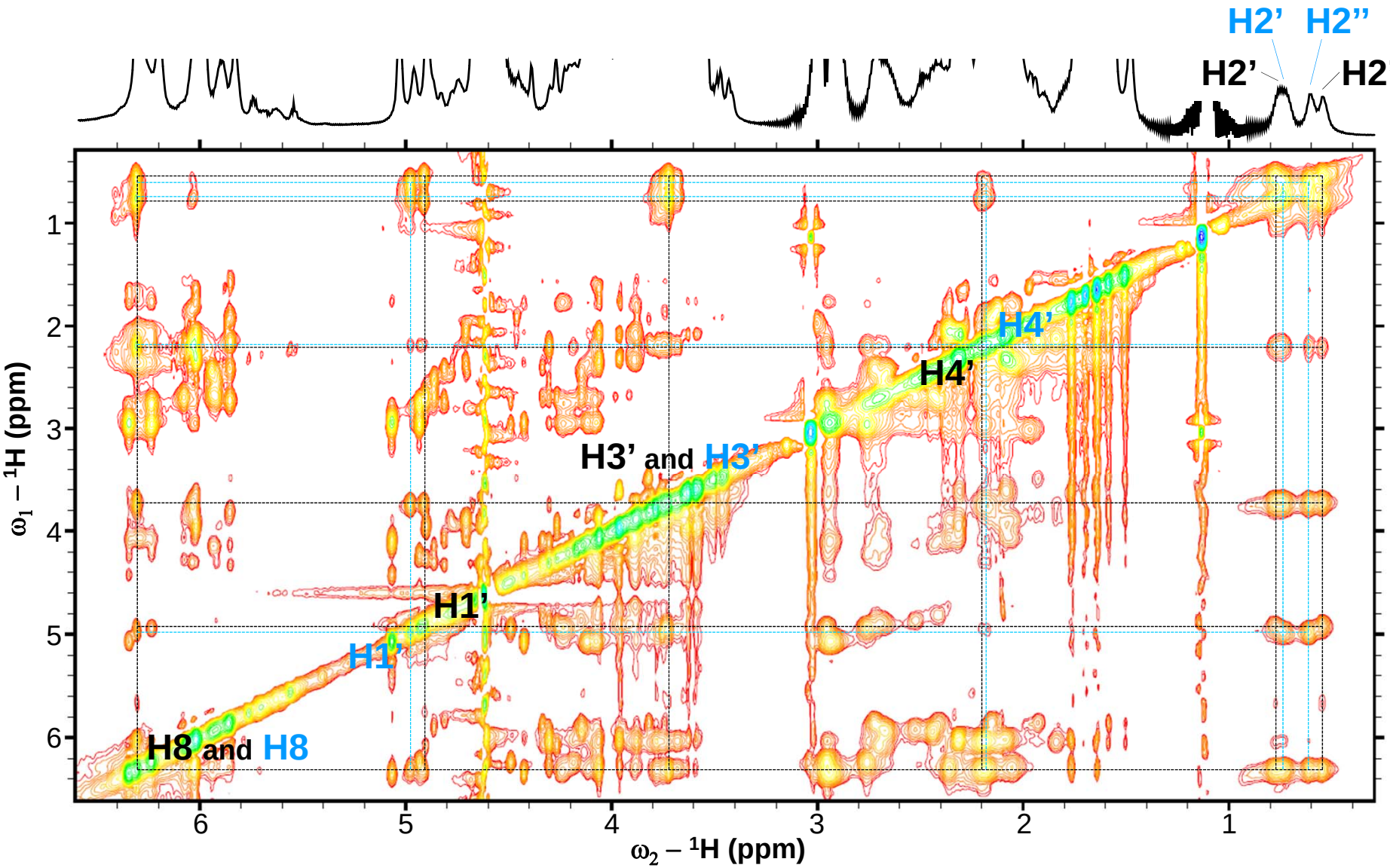

Figure S5. A portion of the NOESY spectrum of the heme(Fe^{3+})-$(d(TTAGGG))_4$ complex in 90%^1H_2O/10%^2H_2O, 300 mM KCl, 50 mM potassium phosphate buffer at pH 9.80 and 25 ºC. A mixing time of 150 ms was used to record the spectrum. Signal assignment of G6 base H8 and ribose H1’, H2’, H2”, H3’, and H4’ proton signals are shown with the spectrum. The G6 ribose H1’, H2’, H2”, and H4’ proton signals appeared as ~1:1 doublet peaks with splitting of 0.02–0.07 ppm (see Figure S6). Two independent NOESY connectivities among the G6 base and ribose proton signals, indicated by blue and black lines, demonstrated that 4-fold (8-fold, considering the DNA dimer as a unit) degeneracy of these protons is removed upon heme(Fe^{3+}) binding to the DNA (see text).

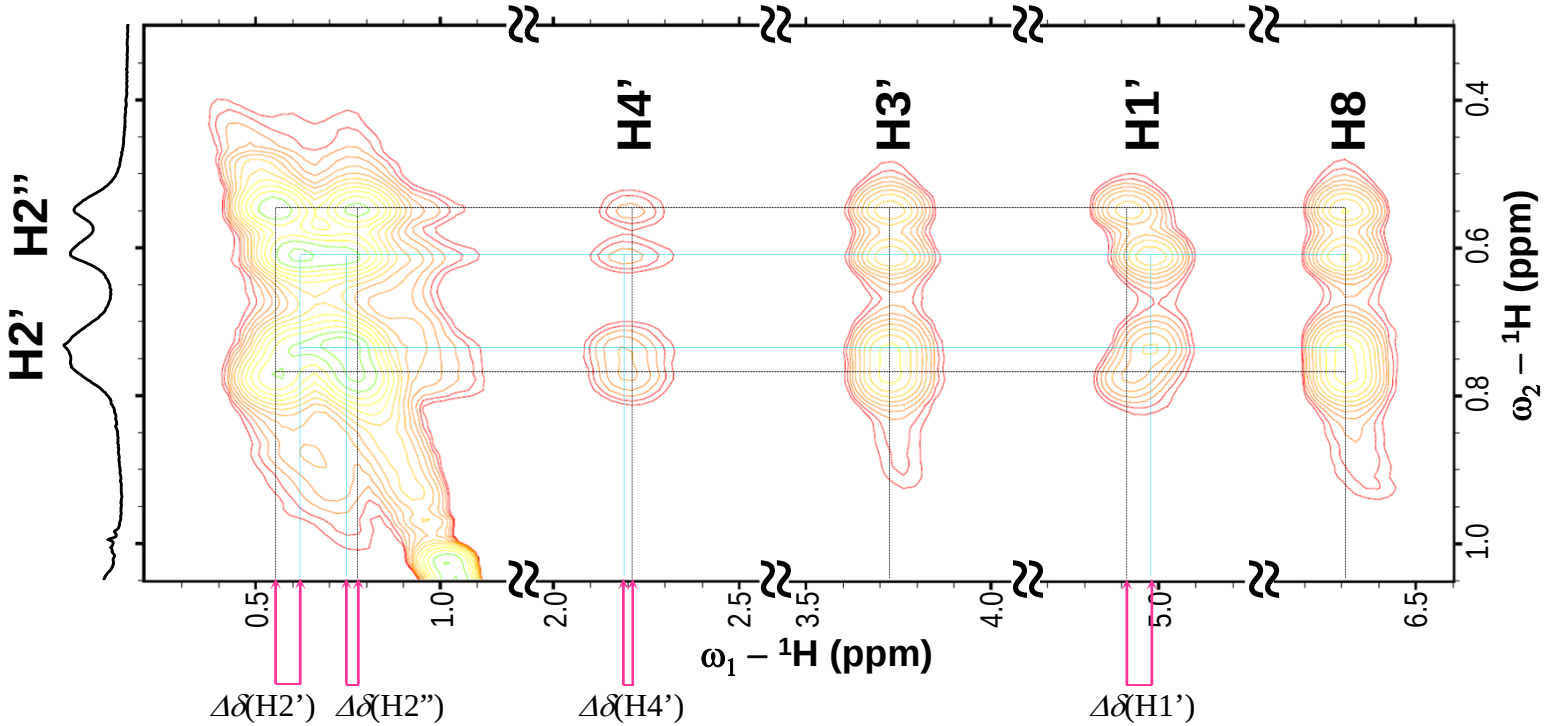

Figure S6. Enlarged displays of the NOESY diagonal- and cross-peaks, 6.60-0.20 ppm (ω_1), 1.05-0.30 ppm (ω_2) in Figure S5. G6 ribose H1’, H2’, H2”, and H4’ proton signals appeared as ~1:1 doublet peaks ($\Delta\delta$(i), i = H1’, H2’, H2”, or H4) with splitting of 0.02 – 0.07 ppm, i.e., 12 – 42 Hz. Two independent NOESY connectivities indicated by blue and black lines demonstrated that degeneracy of these protons is removed upon heme(Fe^{3+}) binding to the DNA, due to the rhombic component of the paramagnetic susceptibility tensor, which is 2-fold symmetric with respect to the heme normal.

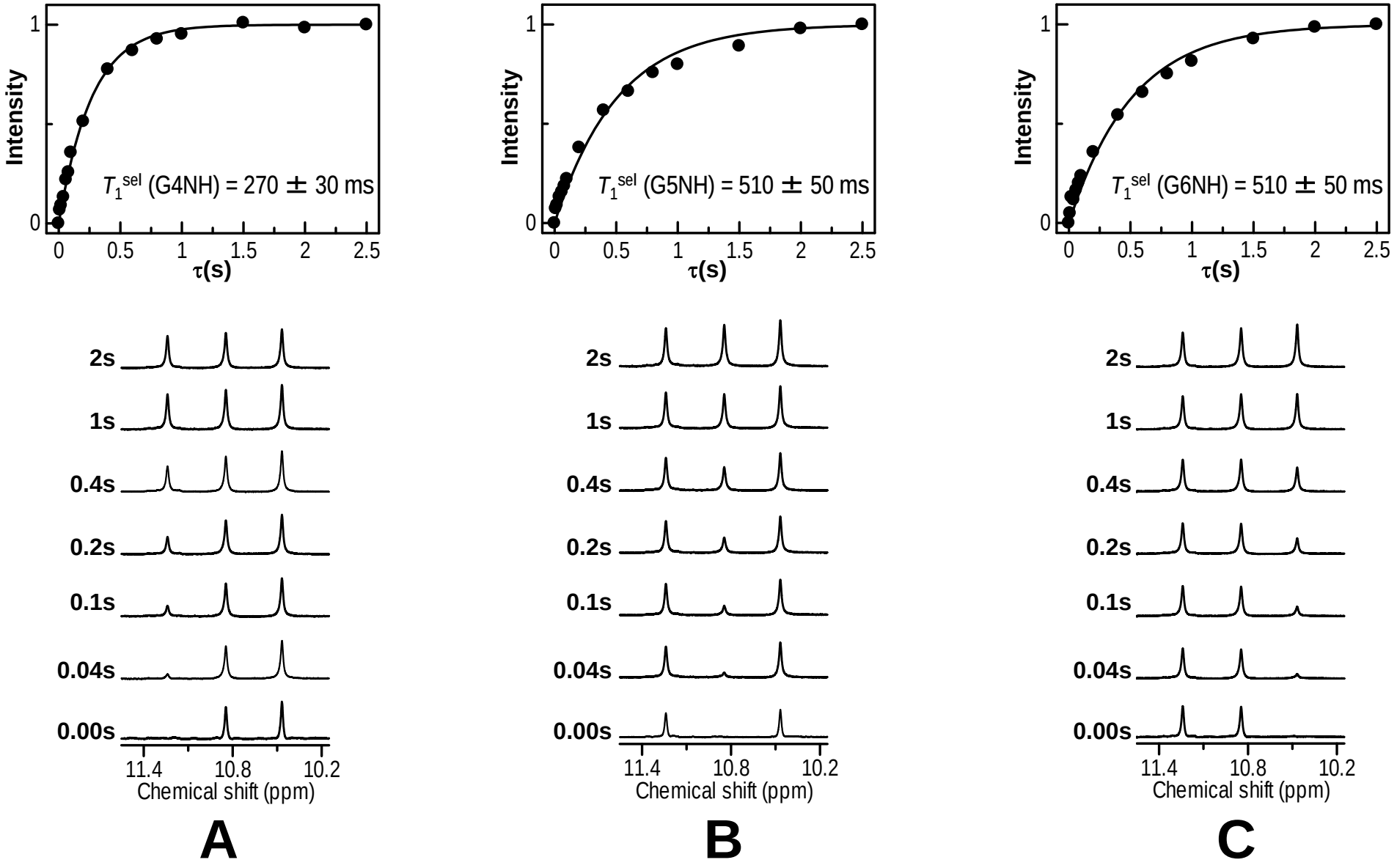

Figure S7. Recovery of the G4NH (A), G5NH (B), and G6NH (C) proton signals of $(d(TTAGGG))_4$ in 90%^1H_2O/10%^2H_2O, 300 mM KCl, 50 mM potassium phosphate buffer at pH 9.80 and 25 ºC, and plots of the signal intensities against the recovery time(τ). The plots were fitted using Intensity(τ) = $(M_{\tau = t}/M_{\tau = 0}) = 1 - \exp(-\tau/T_1^{sel})$, where $M_{\tau = t}$ and $M_{\tau = 0}$ represent signal intensities at τ = t and τ = 0, respectively. Selective T_1^{sel} values of 270 ± 30, 510 ± 50, and 510 ± 50 ms were obtained for G4NH, G5NH, and G6NH, respectively.

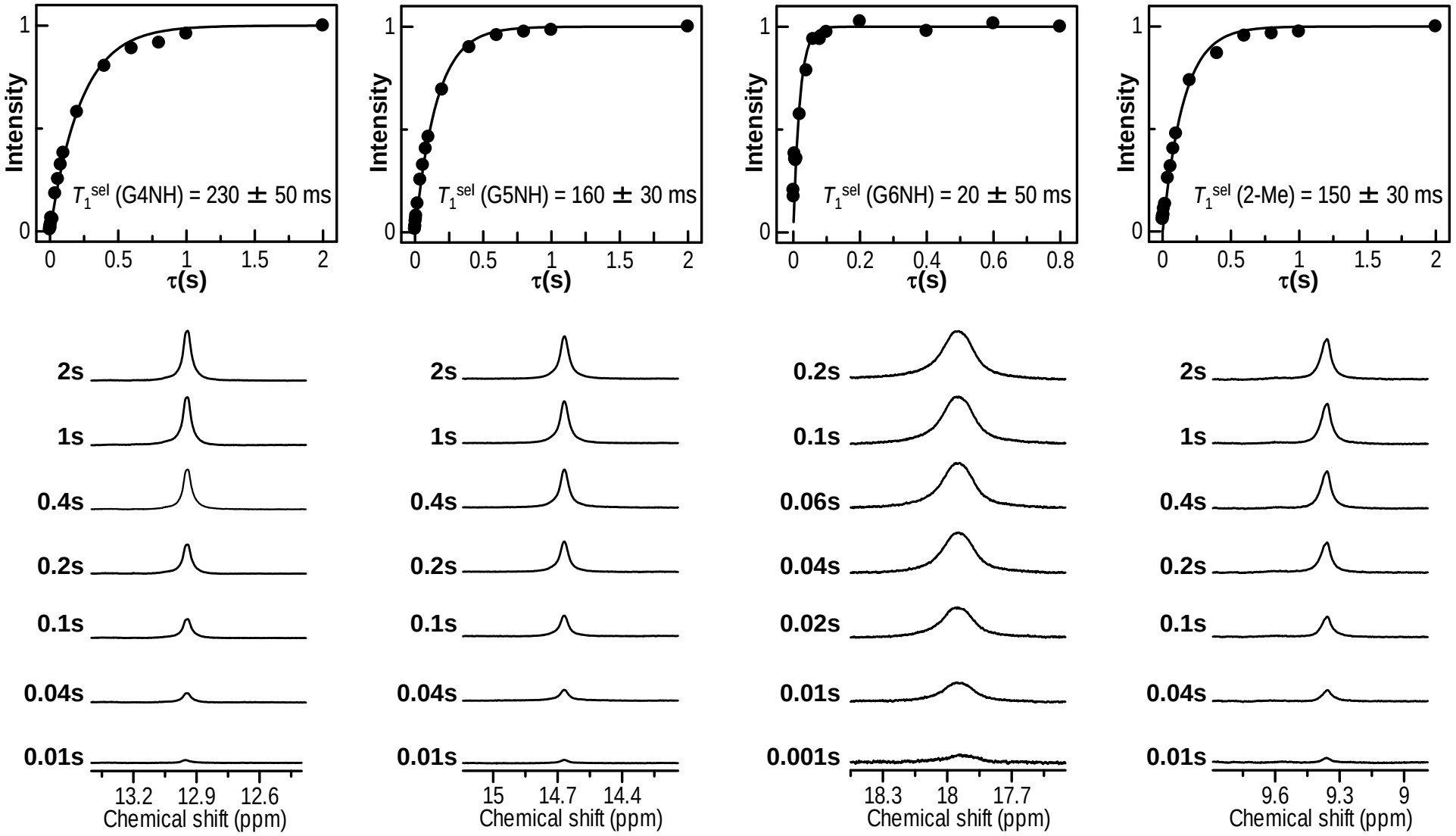

Figure S8. Recovery of the G4NH (A), G5NH (B), G6NH (C), heme 2-Me (D) proton signals of the heme(Fe^{3+})-$(d(TTAGGG))_4$ complex in 90%^1H_2O/10%^2H_2O, 300 mM KCl, 50 mM potassium phosphate buffer at pH 9.80 and 25 ºC, and plots of the signal intensities against the recovery time. The plots were fitted using Intensity(τ) = $(M_{\tau = t}/M_{\tau = 0}) = 1 - \exp(-\tau/T_1^{sel})$, where $M_{\tau = t}$ and $M_{\tau = 0}$ represent signal intensities at τ = t and τ = 0, respectively. Selective T_1^{sel} values of 230 ± 50 , 160 ± 30, 20 ± 50, and 150 ± 30 ms were obtained for G4NH, G5NH, G6NH, and heme 2-Me, respectively.

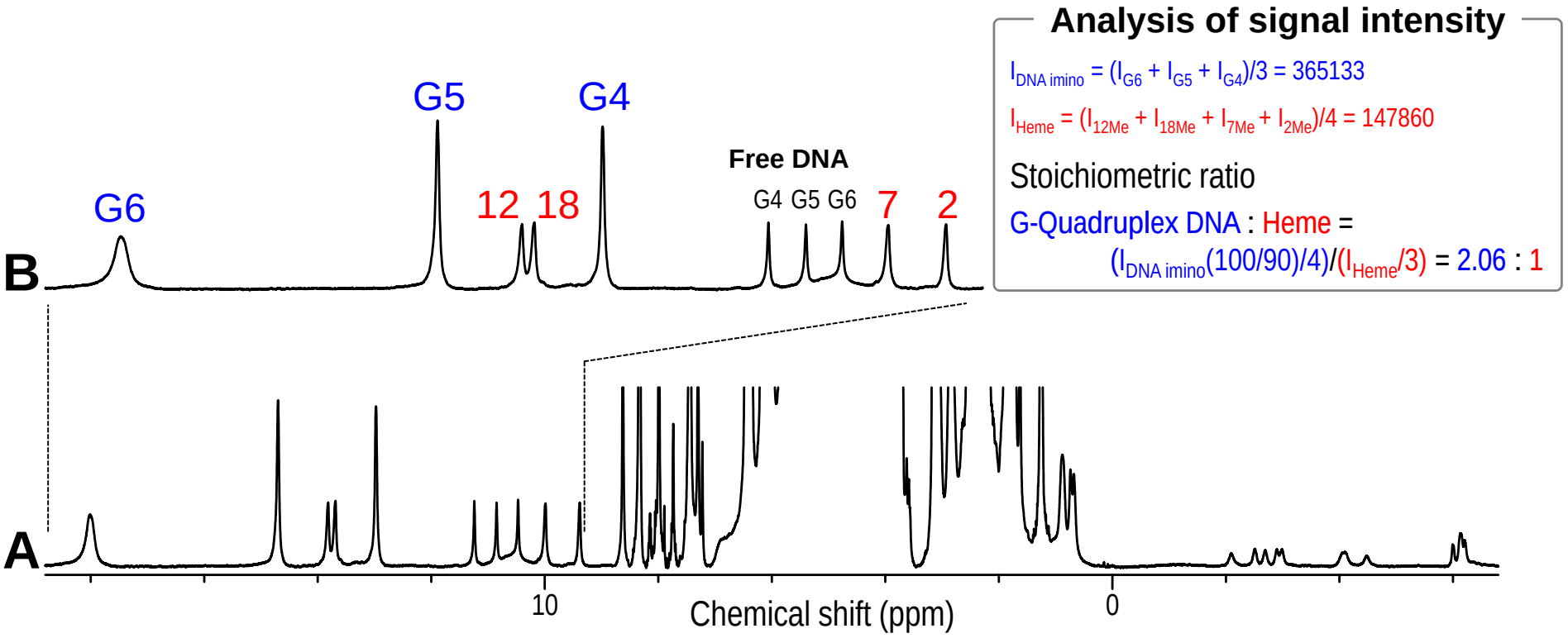

Figure S9. 500 MHz ^{1}H NMR spectrum of G-quadruplex DNA, d(TTAGGG)$_4$, in the presence of a ~0.3 equivalent of heme(Fe^{3+}) in 90%$^{1}H_2O$/10%$^{2}H_2O$, 300 mM KCl, 50 mM potassium phosphate buffer at pH 9.80 and 25 ºC (A), and the downfield-shifted portion, 9.00 – 18.80 ppm, of the spectrum (B). Signal assignments of selected proton signals are shown with trace B, and analysis of the intensities of G-quadruplex DNA imino and heme methyl proton signals of the complex is shown in the inset. The spectrum was recorded with a 35 ppm spectral width, 32k data points, a 2 s relaxation delay, and 29696 transients. The signal-to-noise ratio of the spectrum was improved by apodization, which introduced 0.3 Hz line-broadening.

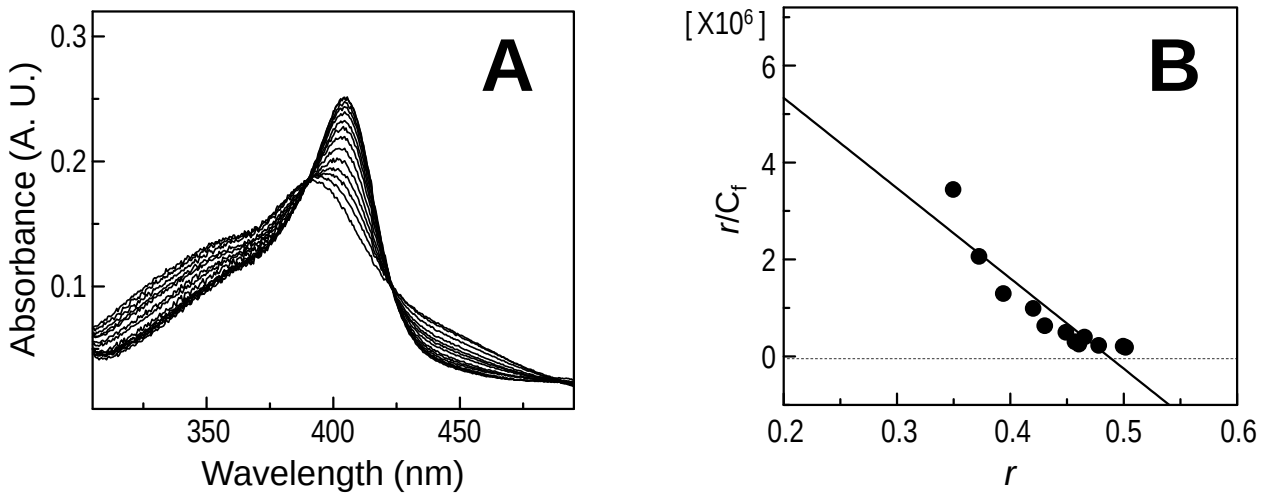

Figure S10. UV-Vis absorption spectra, 305 - 495 nm, of 4.0 μM heme(Fe^{3+}) in the presence of various concentrations of $(d(TTAGGG))_4$ in 300 mM KCl and 50 mM potassium carbonate buffer at pH 10.10 and 25 ºC (A). 0.08 w/v% Triton X-100 and 0.5 v/v% DMSO were added to the solution mixture to prevent heme aggregation. Scatchard plots of the Soret absorbance at 406 nm (B). An association constant of $(9 \pm 5) \times 10^6\ M^{-1}$ and a stoichiometric ratio of 0.5 ± 0.1 between heme(Fe^{3+}) and $(d(TTAGGG))_4$ were obtained.

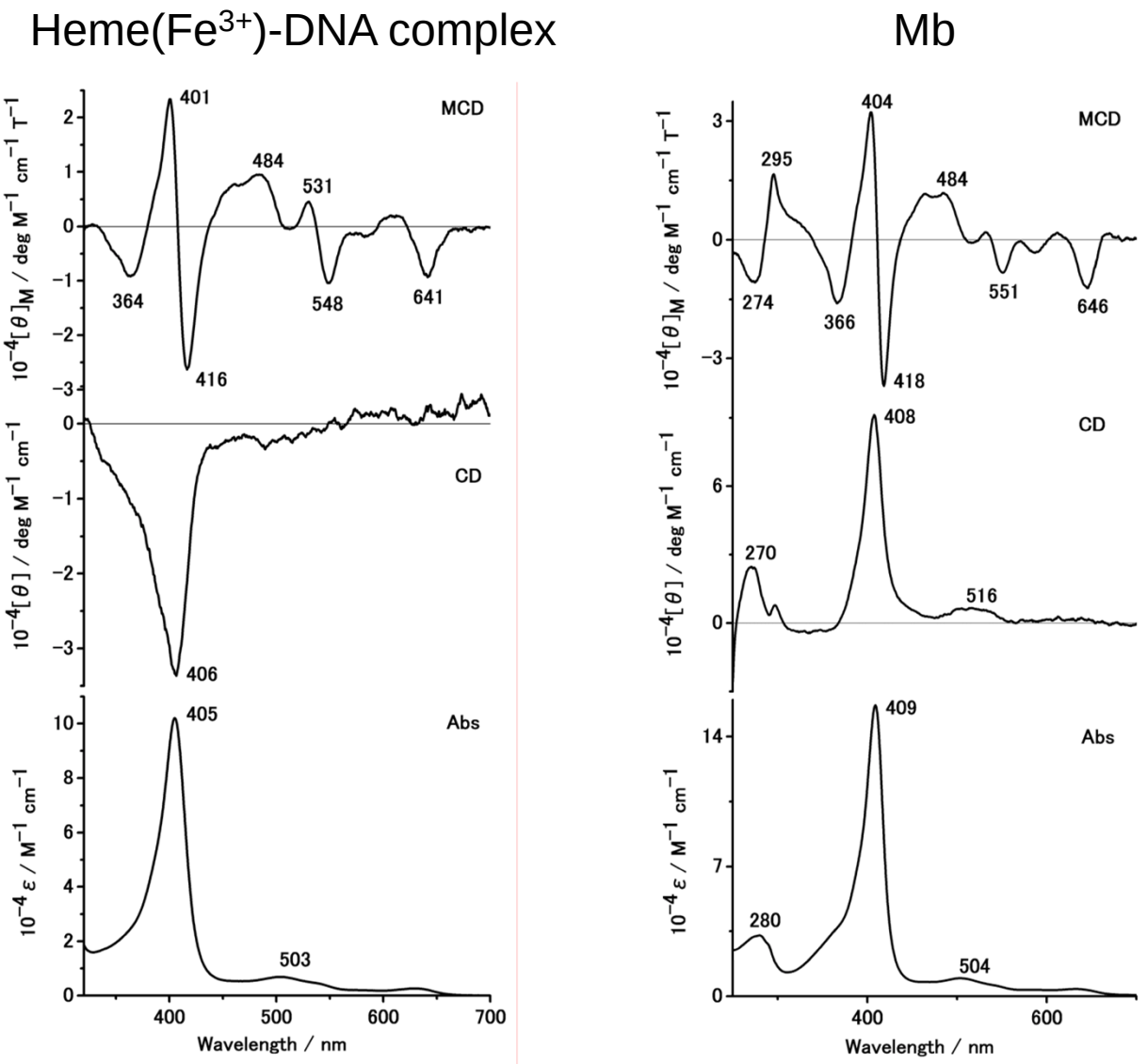

Figure S11. MCD (top), CD (middle), and absorption (bottom) spectra, 305 - 700 nm, of the heme(Fe^{3+})-$(d(TTAGGG))_4$ complex (left) and sperm whale ferric myoglobin (Mb) (right), in 300 mM KCl, 50 mM potassium phosphate buffer at pH 7.00 and 25 ºC. Mb was purchased as a lyophilized powder from Biozyme and used without further purification.

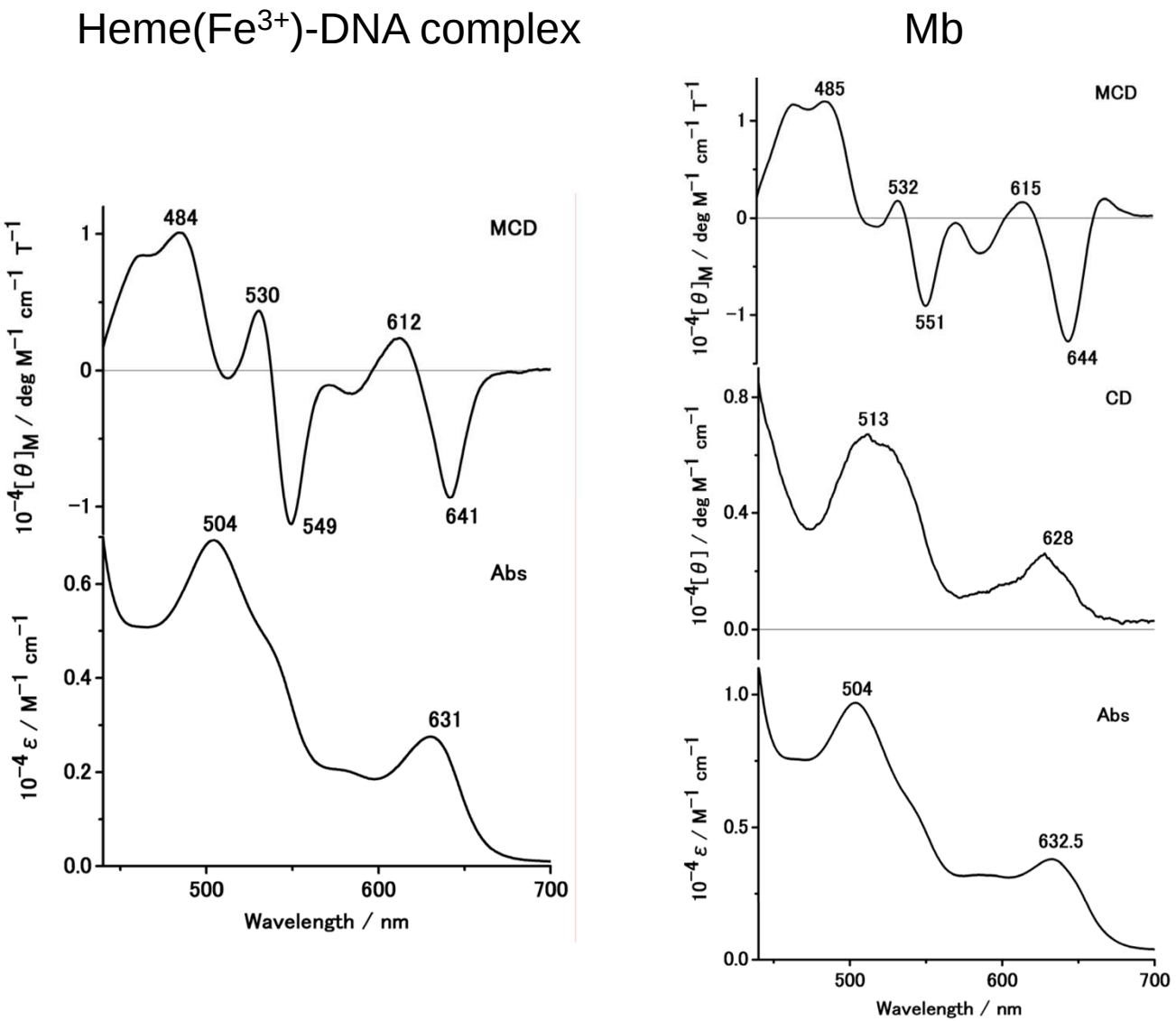

Figure S12. MCD (top), CD (middle), and absorption (bottom) spectra, 440 - 700 nm, of the heme(Fe^{3+})-$(d(TTAGGG))_4$ complex (left) and ferric Mb (right) in 300 mM KCl, 50 mM potassium phosphate buffer at pH 7.00 and 25 ºC. The CD spectrum of the heme-(Fe^{3+})DNA complex is not shown.

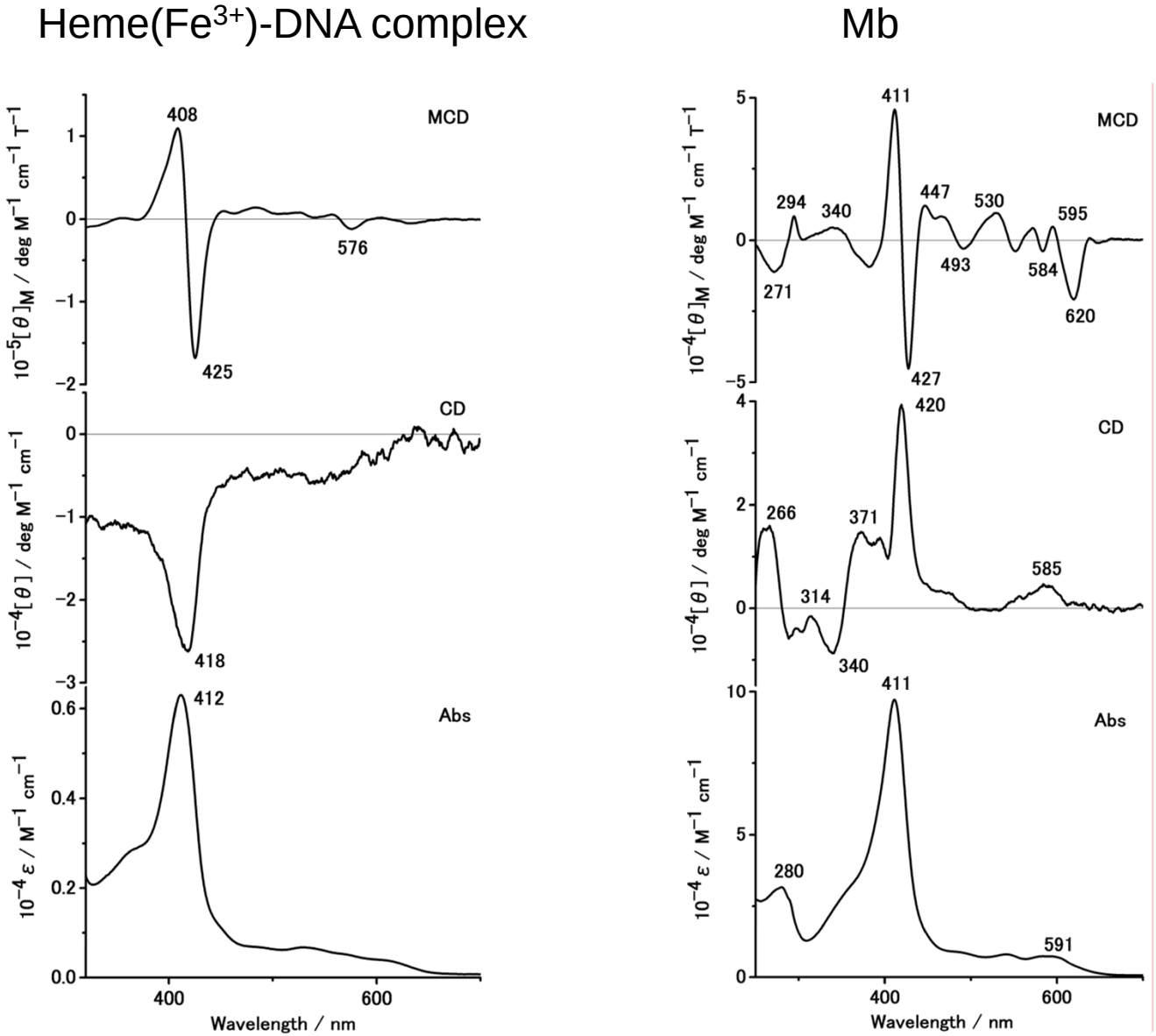

Figure S13. MCD (top), CD (middle), and absorption (bottom) spectra, 305 - 700 nm, of the heme(Fe^{3+})-$(d(TTAGGG))_4$ complex (left) and ferric Mb (right) in 300 mM KCl, 50 mM potassium phosphate buffer at pH 9.80 and 25 ºC.

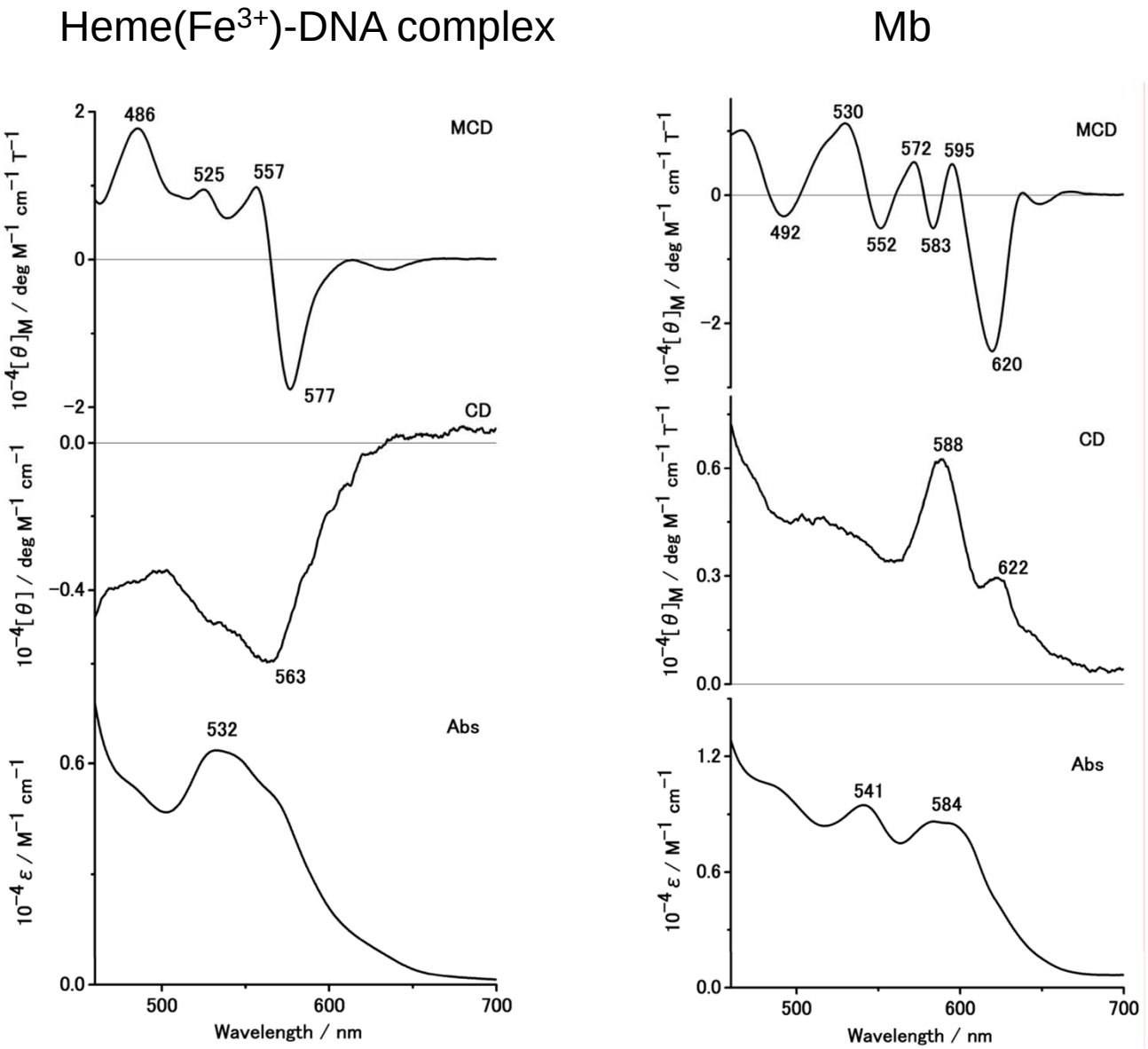

Figure S14. MCD (top), CD (middle), and absorption (bottom) spectra, 440 - 700 nm, of the heme(Fe^{3+})-$(d(TTAGGG))_4$ complex (left) and ferric Mb (right) in 300 mM KCl, 50 mM potassium phosphate buffer at pH 9.80 and 25 ºC.